Proceedings of ICAR 2003
The 11th International Conference on Advanced Robotics
Coimbra, Portugal, June 30 - July 3, 2003

Terrain following preview controller for model-scale helicopters

G. Libório N. Paulino R. Cunha C. Silvestre M. I. Ribeiro

Instituto Superior Técnico
Institute for Systems and Robotics
Torre Norte - Piso 8, Av. Rovisco Pais 1
1046-001 Lisboa, Portugal
{*gui,paulino,rita,cjs,mir*}*@isr.ist.utl.pt*

Abstract

This paper presents the design and performance evaluation of a terrain following controller for model-scale helicopters. The methodology used to develop the tracking controller amounts to augmenting the discrete state space model of the plant with terrain preview data. The terrain information is obtained by applying a 2D reconstruction technique to the measurements taken by a forward looking laser range scanner. The resulting control problem is solved using the discrete time Stochastic Linear Quadratic Regulator where the particular structure of the augmented system is explored to simplify the computation of the feedforward gain matrix. Simulation results obtained with the full nonlinear dynamic model of the Vario X-Treme acrobatic helicopter and the preview controller are presented and discussed.

1 Introduction

Among the many Unmanned Air Vehicle configurations available today, helicopters are one of the most maneuverable and versatile platforms. They can take-off and land without a runway and can hover in place. These capabilities have brought about the use of autonomous model-scale helicopters as highly maneuverable sensing platforms, allowing for the access to remote and confined locations without placing human lives at risk. For these reasons, there is currently great interest in using these platforms in a wide range of applications that include crop spraying, hazardous spill inspection, fire surveillance, pollution monitoring, overhead power cables inspection, bridge and building construction inspection. The existence of high performance terrain following controllers constitutes a fundamental requirement for performing safely many of these tasks.

This paper presents a terrain following controller for model-scale helicopters that takes into account the terrain characteristics ahead of the vehicle. Preview control algorithms have been widely used to improve the overall closed loop performance obtained with limited bandwidth feedback compensators when future information of the commands or disturbances is available. A series of papers on the application of the Linear Quadratic preview control theory to the design of vehicle active suspensions can be found in the literature. Special emphasis should be given to the pioneer work by Tomizuka[8], where the optimal preview control problem is set and solved and the impact of the different preview lengths on the overall suspension performance is discussed. In [7], Prokop et al. present an alternative method that consists of including the disturbance or reference dynamics into the design model and then solving the resulting linear quadratic control problem. The impact of the different actuator bandwidths on the overall system performance is also discussed.

A key question underlying the design of sensor based terrain following control systems is the computation of the terrain elevation data from sensor measurements. In this paper, the technique adopted to perform this task is the so-called "Locus method", described in [4], which exploits the sensor geometry to efficiently build an arbitrary resolution terrain elevation vector.

The preview control system design technique adopted in this paper is in-line with [7] and takes advantage of the arbitrary terrain resolution provided by the locus method [4] to build the future terrain dynamic characteristics vector. This is combined with the linearized longitudinal plane model of the helicopter to obtain the controller synthesis augmented state space realization. The resulting control problem is solved using the discrete time Stochastic Linear Quadratic Regulator where the particular structure of the augmented system is explored to simplify the computation of the feedforward gain matrix.

The design and performance evaluation of the overall closed loop system was done using an accurate self-contained helicopter dynamic model, derived from first-principles, and that is specially tailored for model-scale helicopters [2]. The simulation model, implemented in Matlab, using Simulink and C MEX-file S-functions, includes the rigid body, main rotor flapping, and Bell-Hiller stabilizing bar dynamics and is parameterized for the case of Vario X-Treme acrobatic helicopter.

The paper is organized as follows. Section 2 introduces a general helicopter dynamic model, and presents the simplifications needed to derive control models for both the longitudinal and lateral planes. Section 3 summarizes the design steps leading to development of the terrain following preview controller. Section 4 presents the 2D terrain reconstruction technique. Finally, Section 5 focuses on the implementation of the nonlinear terrain following controller for the Vario X-Treme helicopter, and presents the simulation results obtained with the full nonlinear dynamic model.

2 Helicopter dynamic model

This section presents the dynamic model of a single main rotor and tail rotor helicopter equipped with a Bell-Hiller stabilizing bar, as the Vario X-Treme helicopter depicted in Figure 1. The dynamics of the helicopter are described using a conventional six degree of freedom rigid body model driven by forces and moments that explicitly include the effects of the main rotor, Bell-Hiller stabilizing bar, tail rotor, fuselage, horizontal tailplane, and vertical fin. In rotary-wing aircraft, the main rotor is not only the dominant system, but also the most complex mechanism. It is the primary source of lift, which counteracts the body weight and sustains the helicopter on air. Additionally, the main rotor generates other forces and moments that enable the control of the aircraft position, orientation and velocity. The Bell-Hiller stabilizing bar improves the stability characteristics of the helicopter. The tail rotor, located at the tail boom, provides the moment needed to counteract the torque generated by the aerodynamic drag forces at the rotor hub. The remaining components have less significant contributions and can be described by simpler models. In short, the fuselage produces drag forces and moments and the horizontal tailplane and vertical fin act as wings in forward flight, increasing flight efficiency. A comprehensive study of the helicopter dynamic model can be found in [2], and for an indepth coverage of helicopter flight dynamics, the reader is referred to [5].

Figure 1: *Vario X-Treme helicopter*

The equations of motion were derived, using the following notation:

$\mathbf{p} = \begin{bmatrix} x \ y \ z \end{bmatrix}^T$ - position of the vehicle's center of mass, expressed in an inertial coordinate frame;

$\boldsymbol{\lambda} = \begin{bmatrix} \phi \ \theta \ \psi \end{bmatrix}^T$ - Z-Y-X Euler angles that parameterize locally the orientation of the vehicle relative to the inertial frame;

$\mathbf{v} = \begin{bmatrix} u \ v \ w \end{bmatrix}^T$ - body-fixed linear velocity vector;

$\boldsymbol{\omega} = \begin{bmatrix} p \ q \ r \end{bmatrix}^T$ - body-fixed angular velocity vector.

Figure 2 captures the general structure of the helicopter nonlinear dynamic model. In the figure,

$$\mathbf{x} = \begin{bmatrix} \mathbf{v}^T \ \boldsymbol{\omega}^T \ \mathbf{p}^T \ \boldsymbol{\lambda}^T \end{bmatrix}^T \quad (1)$$

represents the state vector and

$$\mathbf{u} = \begin{bmatrix} \theta_0 \ \theta_{1c} \ \theta_{1s} \ \theta_{tr} \end{bmatrix}^T \quad (2)$$

is the command vector that consists of the main rotor collective input θ_0, main rotor and flybar cyclic inputs θ_{1c} and θ_{1s}, and tail rotor collective input θ_{tr}.

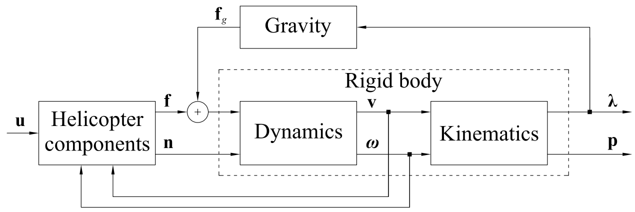

Figure 2: *Helicopter model - block diagram*

2.1 Model Linearization

The control system design, presented in the following sections, is based on the linear models, obtained by linearization of the nonlinear model about specific trimming trajectories, which can be described by

$$\dot{\boldsymbol{\lambda}} = \mathbf{0}, \quad \dot{\mathbf{p}} = \begin{bmatrix} u_c \ 0 \ 0 \end{bmatrix}^T, \quad (3)$$

where u_c is an arbitrary constant. The vehicle is moving at constant speed along a horizontal line trajectory, and has its orientation aligned with that of the inertial frame.

The linearized model describing disturbed motion about a given trimming condition can be written as

$$\dot{\mathbf{x}} = A\mathbf{x} + B\mathbf{u}, \quad (4)$$

where $\mathbf{x}$, $\mathbf{u}$, with an obvious abuse of notation, denote perturbation variables. Still under the small perturbations assumption, the coupling between lateral and longitudinal modes can be neglected, and helicopter motion can be described by two independent lower-order systems. In the case of helicopters, the natural partitioning of the state and input vectors yields

$$\mathbf{x} = \begin{bmatrix} u \ w \ q \ z \ \theta \end{bmatrix}^T \text{and } \mathbf{u} = \begin{bmatrix} \theta_0 \ \theta_{1s} \end{bmatrix}^T,$$

for longitudinal motion, and

$$\mathbf{x} = \left[\, v \;\; p \;\; r \;\; \phi \;\; \psi \,\right]^T \text{ and } \mathbf{u} = \left[\, \theta_{1c} \;\; \theta_{tr} \,\right]^T,$$

for lateral motion.

The full nonlinear model was parameterized for the Vario X-Treme model-scale helicopter. A complete description of the parameters identification can be found in [6].

3 Control system design

This section focuses on the design of a terrain following control system for the Vario X-Treme helicopter, based on the dynamic model presented in Section 2.

The sections that follow summarize the design steps, leading to the development of the longitudinal plane preview controller for the helicopter. The lateral dynamics was stabilized by a simple controller designed using the standard LQR technique.

3.1 Longitudinal controller design

The controller for the longitudinal plane linearization is required to meet the following design specifications: *i) Zero Steady State Error,* in response to constant input commands z_c and u_c for *quasi* flat terrains ($\dot{z}_c \simeq 0$); *ii) Terrain Tracking Requirements,* meaning that the helicopter should be able to track accurately a terrain model described by

$$z_c(t) = \int_{t_0}^{t} s(\tau)\, d\tau, \tag{5}$$

where $\dot{z}_c = s(t)$ is a white noise process that locally represents the terrain slope; *iii) Actuator Bandwidth Requirements,* requiring that the control loop bandwidth for all actuators should not exceed 30 rad/s to ensure that the main and tail rotor command servos would not be driven beyond their normal actuation bandwidth.

The control problem for terrain and longitudinal velocity reference tracking can be stated as follows. Let

$$\mathbf{x_E} = [\, z - z_c \quad \theta \quad u \quad w \quad q \;\; \textstyle\int (z - z_c) \;\; \int u \,]' \tag{6}$$

be the error state vector and consider the continuous time representation of its linearized dynamics

$$\dot{\mathbf{x}}_{\mathbf{E}}(t) = \bar{A}\mathbf{x_E}(t) + \bar{B}\mathbf{u}(t) + \bar{B}_s s(t), \tag{7}$$

where matrices $\bar{A}$ and $\bar{B}$ are easily obtained from (6), and $\bar{B}_s$ is given by

$$\bar{B}_s = [\, -1 \quad 0 \quad 0 \quad 0 \quad 0 \quad 0 \quad 0 \,]' \tag{8}$$

and represents the terrain slope input into the system.

The terrain following controller was obtained by resorting to the solution of the standard Discrete Stochastic Linear Quadratic Regulator problem, [1], where the state and control weighting matrices $Q_{\mathbf{x}}$ and R, respectively, were selected as to minimize the *rms* value of the actuators and terrain tracking errors. The discrete equivalent of the linear continuous model (7) was obtained using the zero-order hold technique. Let T be the sampling time and define $\bar{\mathbf{x}}_{\mathbf{E}}(k)$ and $\bar{\mathbf{u}}(k)$ as the discrete time state and input vectors, respectively. Using this notation, the discrete error dynamics can be written as

$$\bar{\mathbf{x}}_{\mathbf{E}}(k+1) = \Phi\bar{\mathbf{x}}_{\mathbf{E}}(k) + \Gamma_s \bar{s}(k) + \Gamma\bar{\mathbf{u}}(k), \tag{9}$$

where $\bar{s}(k) = \dot{z}_c(kT)$ represents the terrain slope at instant k, $\Phi = e^{\bar{A}T}$, $\Gamma_s = \left(\int_0^T \Phi(\tau)d\tau\right)\bar{B}_s$, and $\Gamma = \left(\int_0^T \Phi(\tau)d\tau\right)\bar{B}$.

3.2 Preview Control

Better terrain tracking performance with limited bandwidth compensators can be achieved by taking into account, in the control law, the terrain characteristics ahead of the helicopter.

In this case, the measurements taken by a forward looking laser range scanner, after being processed, are used to compute the terrain slope which becomes available for feedforward.

The technique used in this paper to develop the tracking controller, is in line with the results presented in [7], and amounts to augmenting the discrete state space model of the plant with a terrain description.

Let the desired terrain preview time $t_p = pT$ be a multiple of the sampling period T and let $\bar{\mathbf{s}}(k) \in \mathbb{R}^{p+1}$ be the vector containing all the preview inputs at instant k

$$\bar{\mathbf{s}}(k) = [\bar{s}(k), \quad \bar{s}(k+1), \ldots \quad \bar{s}(k+p)]'. \tag{10}$$

The discrete time dynamics of vector $\bar{\mathbf{s}}(k)$ can be written as

$$\bar{\mathbf{s}}(k+1) = D\bar{\mathbf{s}}(k) + E\bar{s}(k+p+1), \tag{11}$$

where

$$D = \begin{bmatrix} 0 & 1 & 0 & \cdots & 0 \\ 0 & 0 & 1 & \cdots & 0 \\ \vdots & \vdots & \ddots & \ddots & \vdots \\ 0 & 0 & 0 & \ddots & 1 \\ 0 & 0 & 0 & \cdots & 0 \end{bmatrix}, \quad E = \begin{bmatrix} 0 \\ 0 \\ \vdots \\ 1 \end{bmatrix}.$$

The dynamic system described by (11) represents the time evolution of the terrain slope ahead of the helicopter, that is available for feedforward at instant k.

Combining the dynamic representation of the terrain (11) with (9) yields,

$$\begin{bmatrix} \bar{\mathbf{x}}_{\mathbf{E}}(k+1) \\ \bar{\mathbf{s}}(k+1) \end{bmatrix} = \begin{bmatrix} \Phi & H \\ 0 & D \end{bmatrix} \begin{bmatrix} \bar{\mathbf{x}}_{\mathbf{E}}(k) \\ \bar{\mathbf{s}}(k) \end{bmatrix} + \\ + \begin{bmatrix} 0 \\ E \end{bmatrix} \bar{s}(k+p+1) + \begin{bmatrix} \Gamma \\ 0 \end{bmatrix} \bar{\mathbf{u}}(k), \tag{12}$$

where $H = \begin{bmatrix} \Gamma_s & 0 & 0 & \cdots & 0 \end{bmatrix}$.

Notice that the D matrix is stable and therefore the augmented system (12) preserves the stabilizability and detectability properties of the original plant.

The stationary solution of the Stochastic Linear Quadratic Regulator problem, with performance index matrices $Q = \begin{bmatrix} Q_{\mathbf{x}} & Q_{\mathbf{xs}} \\ Q'_{\mathbf{xs}} & Q_{\mathbf{s}} \end{bmatrix}$ and R, results in a state feedback law that can be expressed as

$$\bar{\mathbf{u}}(k) = \bar{\mathbf{u}}_{\mathbf{x}}(k) + \bar{\mathbf{u}}_{\mathbf{s}}(k) = -[K_{\mathbf{x}} \; K_{\mathbf{s}}] \begin{bmatrix} \bar{\mathbf{x}}_{\mathbf{E}}(k) \\ \bar{\mathbf{s}}(k) \end{bmatrix}, \quad (13)$$

where $K_{\mathbf{x}}$ and $K_{\mathbf{s}}$ represent, respectively, the feedback and the preview gain matrices, and $\begin{bmatrix} S_{\mathbf{x}} & S_{\mathbf{xs}} \\ S'_{\mathbf{xs}} & S_{\mathbf{s}} \end{bmatrix}$ is the symmetric positive definite solution of the discrete algebraic Riccati equation.

Due to the particular structure of the augmented system (12) the control law presents the following properties: *i)* the gains $K_{\mathbf{x}}$ and $K_{\mathbf{s}}$ are given by

$$K_{\mathbf{x}} = (\Gamma' S_{\mathbf{x}} \Gamma + R)^{-1} \Gamma' S_{\mathbf{x}} \Phi \quad (14)$$

$$K_{\mathbf{s}} = (\Gamma' S_{\mathbf{x}} \Gamma + R)^{-1} \Gamma' (S_{\mathbf{x}} H + S_{\mathbf{xs}} D), \quad (15)$$

and are only functions of $S_{\mathbf{x}}$ and $S_{\mathbf{xs}}$; *ii)* matrix $S_{\mathbf{x}}$ is the solution of the algebraic Riccati equation for the system (9), which is independent of the terrain preview; *iii)* matrix $S_{\mathbf{xs}}$ can be computed from $S_{\mathbf{x}}$, see [6] and [7], as follows

$$\begin{aligned} S_{\mathbf{xs}} = {} & [\Phi'_C, (\Phi^2_C)', \cdots, (\Phi^p_C)'] S_{\mathbf{x}} \Gamma_s + \\ & [Q_1, \Phi'_C Q_1 + Q_2, ..., \sum_{j=1}^{p} (\Phi^{p-j}_C)' Q_j], \end{aligned}$$

where $\Phi_C = [\Phi - \Gamma K_{\mathbf{x}}]$ is the closed loop dynamic matrix and Q_j denotes the *jth* column of matrix $Q_{\mathbf{xs}}$. Notice that the last property can be of extreme importance to compute the controller gain matrices for large preview windows, namely $p > 50$.

In the design example presented in the paper, the sampling period was chosen as $T = 0.02$s, the controller design weighting matrices were set to $R = I$, $Q_{\mathbf{x}} = \mathrm{diag}(0.2,\ 0.1,\ 0.1,\ 0.1,\ 0.1,\ 0.02,\ 0.02)$, $Q_{\mathbf{xs}} = 0$, $Q_{\mathbf{s}} = 0$, and $p = 100$ which corresponds to previewing the terrain two seconds ahead.

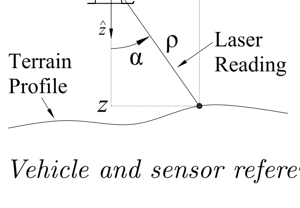

Figure 3: *Vehicle and sensor reference frames*

4 Terrain Preview

Different range sensing techniques can be used to obtain the terrain elevation measurements. In the present case study, a 2D laser range scanner was used. To compute the terrain elevation data, z_c, from the simulated sensor measurements, a simplification of a 3D reconstruction technique was implemented. This technique, named the Locus Method, see [4], is applied on the sensor space taking advantage of the uniformly spaced data to efficiently compute the terrain elevation.

Each sensor reading returns a pair (ρ, α) of the measured range, ρ, and scanning angle, α. Without loss of generality assume that the sensor scanning plane is coincident with the xoz plane of the vehicle body fixed frame, and let $\alpha = 0$ when the beam is aligned with the vertical and pointing downwards, see Figure 3. In the vehicle frame, the x, z coordinates of a generic terrain point are expressed as

$$\begin{aligned} x &= \rho \sin \alpha \\ z &= \rho \cos \alpha, \end{aligned} \quad (16)$$

see Figure 3.

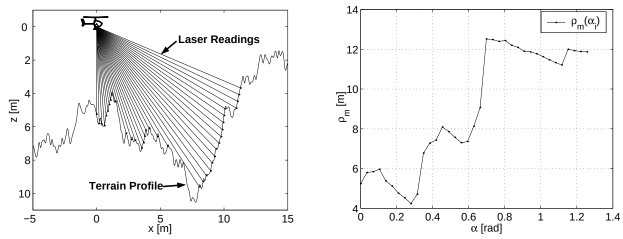

(a) Curve in (x,z) vehicle coordinates (b) Curve $\rho_m(\alpha)$ in sensor coordinates

Figure 4: *Curves obtained from simulated laser readings*

Given a laser scan line, the terrain reconstruction problem at hand consists of finding the terrain elevation coordinate z for a set of points equally spaced in x. The technique used follows [4] and can be briefly described as follows: For $\mathcal{X}$, a given set of x coordinates, do:

1 - obtain the curve $\rho_m(\alpha)$ from the proper interpolation in α of the scanning measurements, Figure 4,

2 - for the current $x_i \in \mathcal{X}$ compute the image of the straight line $x = x_i$ on the ρ, α plane, i.e. curve $\rho_x(\alpha) = \frac{x_i}{\sin \alpha}$, Figure 5,

3 - find the pair (ρ_i, α_i) for which the two curves intersect,

4 - compute the respective elevation, $z_i = \rho_i \cos(\alpha_i)$,

and repeat 2 to 4 for all $x_i \in \mathcal{X}$.

With the present method, changing the reconstruction resolution can be easily obtained by redefining the set $\mathcal{X}$. This fact turns out to be of utmost importance,

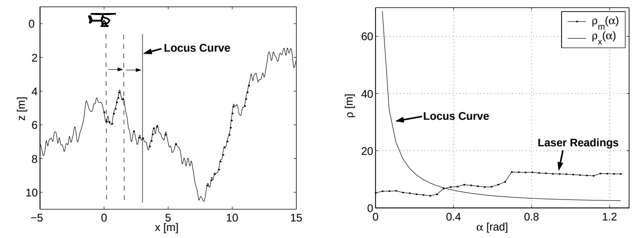

(a) Curves in (x,z) vehicle coordinates (b) Curves in (ρ,α) coordinates

Figure 5: *Locus method, intersection of $\rho_m(\alpha)$ with $\rho_x(\alpha)$*

since it allows to naturally redefine the controller visibility distance, as a function of the vehicle velocity, preserving the dimension of the preview input vector. This is simply obtained by setting $x_k \in \mathcal{X}$ to $x_k = kTu_c$. Notice that the space sampling resolution is a function of the vehicle's speed, u_c, and the sample interval, T. An example of this property is represented in Figure 6, where two terrain reconstructions were obtained for two different velocity values. From the figure it becomes clear how the vehicle velocity has an impact on the visibility distance. The limit case $u_c \to 0$ results on a pure hovering maneuver where the preview samples are taken from the terrain below the helicopter.

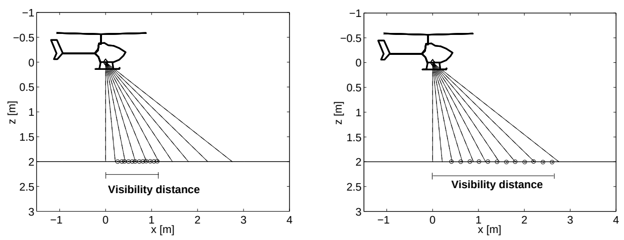

(a) $u_c = 4\,ms^{-1}$ (b) $u_c = 10\,ms^{-1}$

Figure 6: *Terrain elevation for $x = kTu_c$*

Another advantage of the method is the fact that it implicitly takes care of occlusions due to the terrain geometry. The Locus Method provides an upper-bound for the elevation shadowed by the obstacle, as depicted in Figure 7.

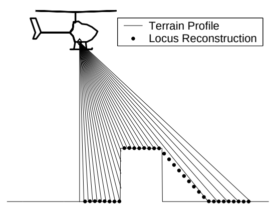

Figure 7: *Occluded areas in presence of obstacles*

The terrain slope vector needed to feed the tracking controller is obtained by a numerical backward Euler derivative of the terrain elevation vector.

5 Nonlinear controller implementation and simulation results

This section describes briefly the controller implementation technique and assesses the performance of the longitudinal closed loop system along a typical terrain. The implementation of the resulting controller was done by using the D-methodology described in [3], which guarantees the following fundamental linearization property: the linearization of the nonlinear feedback control system about each equilibrium trajectory preserves the internal, as well as the input-output, properties of the corresponding linear closed loop designs. This methodology moves all integrators to the plant input, and adds derivators where they are needed to preserve the transfer functions, making straightforward the implementation of anti-windup schemes, see Figure 8. Furthermore, the input trimming values are naturally provided by the integrator block, which is a major issue in this application where the constant terms present in the model have to be compensated.

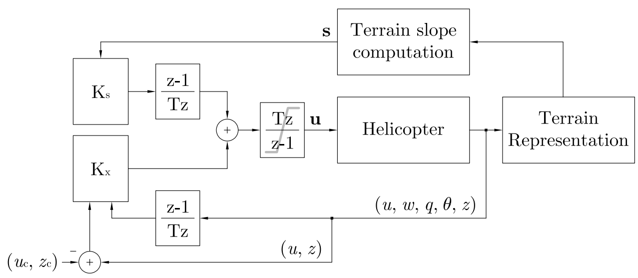

Figure 8: *Longitudinal closed loop system.*

The results of the simulation presented in Figures 9-11 were obtained with the nonlinear closed loop system represented in Figure 8 that includes the nonlinear dynamic model of the Vario X-Treme helicopter together with the D-implementation of the longitudinal plane controller. During the maneuver, the lateral plane of the vehicle was stabilized using a simple LQR regulator acting on the longitudinal cyclic and on the tail rotor.

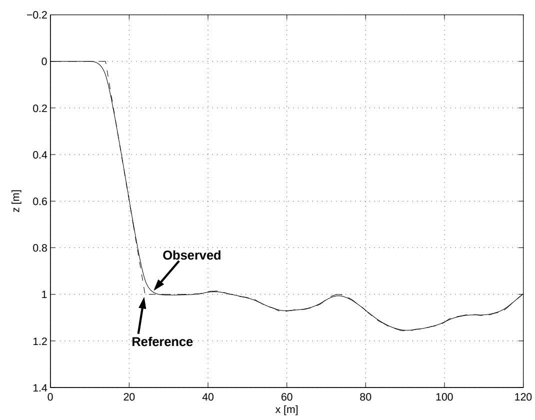

Figure 9: *Closed loop step response, 2D view, vertical plane*

The maneuver performed at constant forward speed of 2.0 m/s consists of firstly tracking a negative ramp followed by random terrain profile, see Figure 9. As depicted in Figure 11, during the first 30 s of the maneuver, the actuation variables θ_0, θ_{1s}, that correspond to the collective and lateral cyclic, change to impart the desired descending rate to the vehicle.

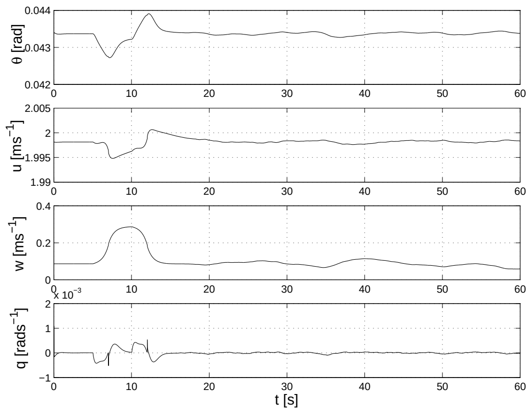

Figure 10: *Longitudinal states for the nonlinear model*

The remaining actuation variables that are the longitudinal cyclic, θ_{1c}, and the collective tail rotor, θ_{tr}, commanded by the lateral controller, react as to compensate for the model coupling, see Figure 11. As the vehicle enters on the random terrain, small variations on the actuation are required to keep the helicopter close to the desired trajectory. It is important to remark that, due to the preview action, the controller behaves in advanced enabling the closed loop system to achieve good terrain tracking performance even with limited bandwidth feedback compensators.

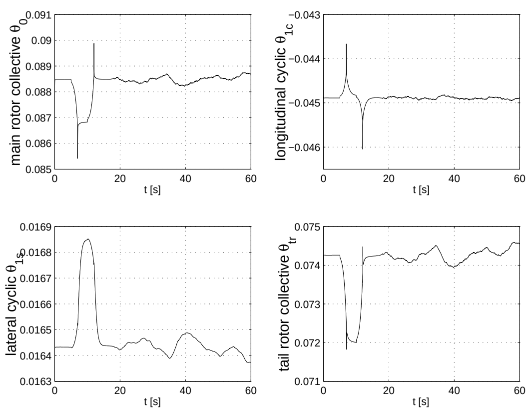

Figure 11: *Command inputs*

6 Conclusions

This paper presented the design and performance evaluation of a laser based terrain following control system for autonomous helicopters. The technique described achieves good terrain following performance with limited bandwidth compensators by taking into account, in the control law, the terrain characteristics ahead of the helicopter. The control problem was cast and solved in the framework of discrete-time stochastic linear quadratic regulator and a methodology to obtain the terrain preview information from the laser range scanner data was introduced. The success of the design procedure was evaluated in simulation with a full nonlinear model of the Vario X-Treme helicopter. Future work will focus on finding new error spaces able to naturally exploit the particular dynamic characteristics of the helicopter in its whole flight envelope, addressing the development of feedback/feedforward control laws to achieve good tracking characteristics in high demanding maneuvers.

Acknowledgments

This work was partially supported by the FCT Programa Operacional da Sociedade de Informação (POSI) in the frame of QCA III and by the POSI/SRI/41938/2001 ALTICOPTER project.

References

[1] Anderson B. D. O., Moore J. B., *Optimal Control, Linear Quadratic Methods*, Prentice Hall, New Jersey, USA, 1990.

[2] Cunha R., *Modeling and control of an autonomous robotic helicopter*, MSc Thesis, Department of Electrical and Computer Engineering, Instituto Superior Técnico, 2002.

[3] Kaminer I., Pascoal A., Khargonekar P., Coleman E., "A Velocity Algorithm for the Implementation of Gain-Scheduled Controllers", *Automatica*, 31(8):1185–1191, 1995.

[4] Kweon I., Kanade T., "High Resolution Terrain Map from Multiple Sensor Data", in *IEEE Trans. on Patt. Anal. Machine Intell.*, vol. 14, no.2, pp. 278-292, February 1992.

[5] Padfield G.D., *Helicopter Flight Dynamics*, American Institute of Aeronautics and Astronautics, Education Series, 1996.

[6] Paulino N., Libório G. *Distributed Control System for Stabilization and Flight Control at Low Altitude for a Scale Helicopter* (in Portuguese), Final Year Project, Instituto Superior Técnico, 2002.

[7] Prokop G., Sharp R. S., "Performance enhancement of limeted bandwith active automotive suspensions by road preview", *CONTROL 94*, University of Warwick, 1994, pp. 173-182 (IEEE Publication No. 389)

[8] Tomizuka, M., "Optimum Linear Preview Control with Application to Vehicle Suspension"-Revisited, in *ASME, Journal of Dynamic Systems, Measurement, and Control*, 98, pp 309-315, 1976.